

## Electronic Supplementary Material

# Liquid-Solid Spinodal Decomposition Mediated Synthesis of Sb<sub>2</sub>Se<sub>3</sub> Nanowires and Their Photoelectric Behavior.

Yong Hun Kwon<sup>a</sup>, Myoungho Jeong<sup>b,c</sup>, Hyun Woo Do<sup>a</sup>, Jeong Yong Lee<sup>b,c</sup>, and Hyung Koun Cho<sup>\*a</sup>

<sup>a</sup>School of Advanced Materials Science and Engineering, Sungkyunkwan University, 2066 Seoburo, Jangan-gu, Suwon, Gyeonggi-do, 440-746, Republic of Korea

<sup>b</sup>Center for Nanomaterials and Chemical Reactions, Institute for Basic Science (IBS), 291 Daehak-ro, Yuseong-gu, Daejeon, 305-701, Republic of Korea

<sup>c</sup>Department of Materials Science and Engineering, Korea Advanced Institute of Science and Technology (KAIST), 291 Daehak-ro, Yuseong-gu, Daejeon, 305-701, Republic of Korea

# 1. Determining the applied potential

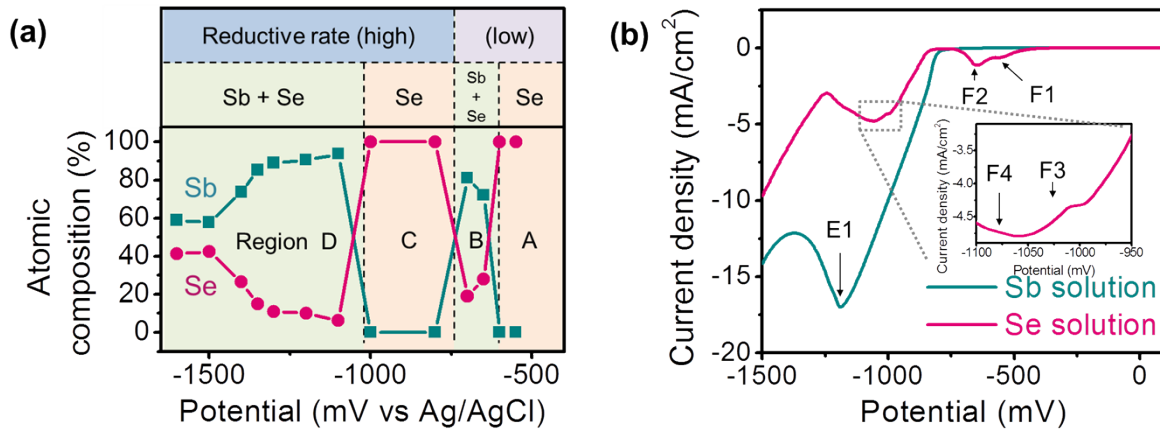


**Figure S1.** (a) EDS results of the electrodeposited precursors at various potentials and (b), linear sweep voltammetry results of the pure Sb and Se solutions.

To determine the appropriate potential for the high reductive rate and co-deposition of Sb and Se, electrodeposition was processed at various potentials ranging from -550 to -1600 mV, and the compositions of samples were measured by EDS, as shown in Fig. S1(a). Metal precursors were deposited until the applied charges accumulated to 1 C/cm<sup>2</sup>. Less than 2 min was required at the potential more negative than -800 mV, but the deposition time at the potential more positive than -700 mV was limited to an hour due to the low reductive rate. Consequently, the applied potential was categorized into low and high reductive rates. In addition, according to the EDS results, these potentials could be divided into four regions in total, depending on the composition of the incorporated Sb and Se elements (regions A, B, C, and D); regions A and B and regions C and D corresponded to low and high reductive rates, respectively, as shown in Fig. S1(a). In the region A (potential of around -500 mV), almost pure Se component was detected on the surface. On the other hand, region B revealed Sb-rich metal precursors with considerably reduced Se composition (Sb+Se). This trend was also repeated in the high reductive rate (regions C and D). At less than -

800 mV (region C), the almost pure Se film was observed again; and finally, the mixed precursors consisting of the Sb and Se elements were deposited in region D (negative potential of more than -1100 mV). Moreover, in the region D, Sb ratio was decreased with respect to potential changes from -1100 to -1500 mV. Interestingly, it is saturated at 58 at % (Sb) and 42 at % (Se); and this is quite similar to the ratio of ionic mole concentration in electrolyte, which indicates the presence of diffusion controlled reaction in the region D. Therefore, it is expected that Sb and Se co-deposition can be successfully achieved with high reductive rate of potential region D.

Typically, the composition variation depending on the applied potential was related to the electrochemical reaction which takes place at the interface of an electrode, ionic conductor, and the electrolyte<sup>S1</sup>. Thus, to investigate in detail the chemical reaction in region D, current responses of a working electrode in the aqueous solution including Sb and Se ionic conductors were observed by linear sweep voltammetry within the range from 100 to -1500 mV, as shown in Fig. S1(b), where voltammetry sweep rate was 20 mV/sec. For the Sb synthesis, aqueous solution containing 0.055 M  $K(SbO)C_4H_4O_6 \cdot 0.5H_2O$  and 1 M  $NH_4Cl$  (ammonium chloride) were used. Se solution contained 0.045M  $H_2SeO_3$  (selenous acid) and 1 M  $NH_4Cl$  (ammonium chloride). The pH for Sb and Se solution was around 3.8 and 1.8, respectively. Sweep rate during the analysis was 20 mV/sec. As a result, one distinct peak (E1) associated with equation (1) was observed in Sb solution<sup>S2, S3</sup>.



On the contrary, for the Se solution, four distinguishable peaks were observed due to the complex reaction of Se (IV). According to previous reports, the electrochemical reaction of Se (IV) in acidic medium can be suggested as following equations, depending on applied potential<sup>S2, S3</sup>.





The equations (2) and (3) correspond to the bulk Se deposition and the reduction of Se (IV) to Se (II-), respectively. If acid solution has sufficient Se (IV) concentration, the Se (II-) induced by Eq. (3) also contributes to the reaction for Se deposition via equation (4). On the other hand, the equation (5) induces the stripping of Se from the substrate. In our results, the reactions corresponding to Eq. (2) and Eq. (3) were confirmed as F1 and F2 peaks in low reductive rate [Fig. S1(b)]. The F4 can be assigned to Eq. (5) for the stripping of Se from the ITO surface. In addition, the F3 is known as the trailing edge, which indicates a balance between the mass loss induced by Eq. (5) and redeposition through Eq. (4)<sup>S2, S3</sup>.

Considering these basic current responses, the potential of the region D is sufficient for the removal of Se and induces the effective deposition of Sb component, resulting in Sb and Se mixed composition. Furthermore, as reported by Y. Lai et al., the sufficient  $\text{SbO}^+$  near the surface strongly inhibits the reduction of Se (IV) to Se (0)<sup>S2, S4</sup>. Thus, it is considered that overall process within the potential range from -1100 to -1300 mV reinforces the deposition of Sb. When the applied potential was negatively shifted, Sb deposition was partially determined by diffusion process due to the enough overpotential<sup>S5-S7</sup>. It is certain that more negative potential induces more stripping of Se, but also depletes the  $\text{SbO}^+$  near the surface of ITO electrode. As a result, the stripping and deposition of Se could coexist, and the final composition would be determined by a balance between these two processes. The EDS results of Fig. S1(a) experimentally show that the amount of the Se deposition is more dominant than stripping of Se. Therefore, Sb and Se could be effectively co-deposited in the potential region D, and this potential also corresponds to high reductive rate showing fast deposition. Consequently, in this experiment, -1400 mV belonging to the region D is selected for deposition potential. At this potential, Sb/Sb-Se stacked structure was clearly confirmed due to the changes in

chemical reaction from Sb deposition to Sb-Se co-deposition (Sb deposition occurred until depletion of  $\text{SbO}^+$ ).

## 2. Estimation for the thermodynamic reduction potential of the $\text{Sb}_2\text{Se}_3$

For the photocathode in the photoelectrochemical cells, the chemical resistance should be retained from the photocorrosion under illumination to perform long-term operation<sup>S8, S9</sup>. It is known that this photocorrosion is induced by the photogenerated electrons ( $e^-$ ) rather than the water. To estimate the stability of the compound semiconductors for PEC, S. Chen and L.W. Wang proposed the calculation method based on the following reaction<sup>S9</sup>.



Here, MX (e.g., M = Cu, Sb, X = O, Se) is the compound semiconductor. When the reaction is in equilibrium, the corrosion does not occur; but at the higher potential, the semiconductor will be corroded. This potential is called thermodynamic reduction potential,  $\phi^{\text{re}}$ , and it is possible to be calculated by using the changes in Gibbs free energy. For  $\text{Sb}_2\text{Se}_3$ , we calculated the  $\phi^{\text{re}}$  relative to the  $\phi(\text{H}^+/\text{H}_2)$  using following equation<sup>S9</sup>.



$$\phi^{\text{re}} - \phi(\text{H}^+/\text{H}_2) = -\Delta G/6eF \quad (8)$$

As a result, thermodynamic reduction potential was estimated as -0.3 V, which indicates the stable characteristic against the photocorrosion. The value of Gibbs free energy is referred to the thermochemical data of pure substances<sup>S10</sup>.

### 3. Supplementary data

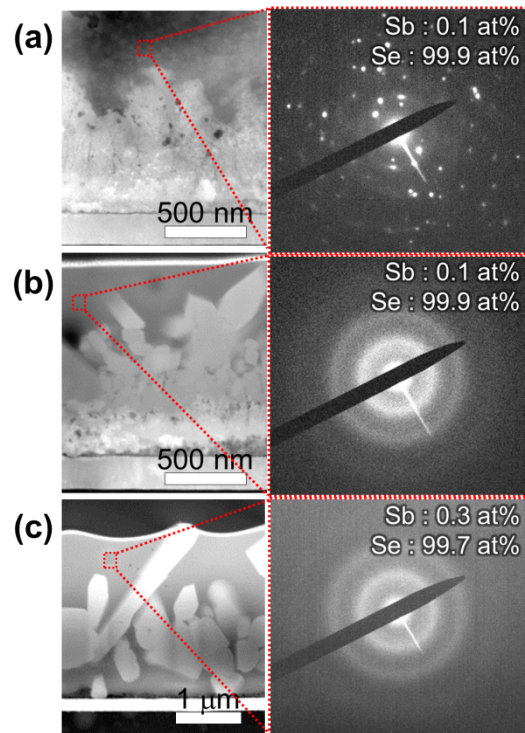


**Figure S2.** (a) 423, (b) 523, and (c) 623 K [the same samples with Fig. 4(c)]. DPs were obtained from the area indicated by red rectangles in the top regions. It was confirmed that polycrystallized Se was changed to amorphous phase above the 523 K, and amorphous Se covered the  $\text{Sb}_2\text{Se}_3$  nanowires. This indicates that the Se was melted by the annealing process and remained as the amorphous phase due to the rapid cool-down.

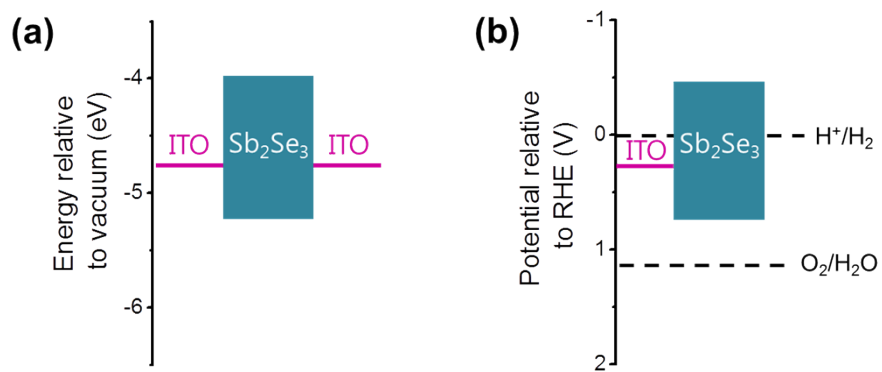


**Figure S3.** (a) ITO/ $\text{Sb}_2\text{Se}_3$ /ITO and (b) ITO/ $\text{Sb}_2\text{Se}_3$ /water. Schottky barrier between the ITO and  $\text{Sb}_2\text{Se}_3$  can limit the carrier conduction at the low voltage.

## References

- S1. M. Paunovic and M. Schlesinger, *Fundamentals of electrochemical deposition*, Wiley, New York, 1998.
- S2. Y. Lai, C. Han, X. Lv, J. Yang, F. Liu, J. Li and Y. Liu, *J. Electroanal. Chem.*, 2012, **671**, 73.
- S3. C. Wei, N. Myung and K. Rajeshwar, *Journal of Electroanalytical Chemistry*, 1994, 109.
- S4. Y. Lai, Z. Chen, C. Han, L. Jiang, F. Liu, J. Li and Y. Liu, *Appl. Surf. Sci.*, **2012**, **261**, 510.
- S5. A. R. Despic and K. I. Popov, *J. Appl. Electrochem.*, 1971, **1**, 275.
- S6. E. Ben-Jacob, G. Deutscher, P. Garik, N. D. Goldenfeld and Y. Lareah, *Phys. Rev. Lett.*, 1986, **57**, 1903.
- S7. F. Liu, C. Huang, Y. Lai, Z. Zhang, J. Li and Y. Liu, *J. Alloy. Compd.*, 2011, **509**, L129.
- S8. H. Gerischer, *J. Electroanal. Chem. Interfacial Electrochem.*, 1977, 82, 133.
- S9. S. Chen and L.-W. Wang, *Chem. Mater.*, 2012, **24**, 3659.
- S10. I. Barin, in *Thermochemical Data of Pure Substances*, VCH, Weinheim, 1995, DOI: 10.1002/9783527619825.ch12i, ch. 12.